Surface tension effects on the behavior of two cavities near a rigid wall

Zhen-yu Zhang* and Hui-sheng Zhang†
Department of Mechanics and Engineering Science, Fudan University, Shanghai 200433, China
(Received 28 October 2004; revised manuscript received 28 March 2005; published 7 June 2005)

Surface tension effects on the behavior of two initially spherical cavities growing and collapsing axisymmetrically above and near a rigid wall are investigated numerically by boundary integral method. The numerical simulations are performed for different dimensionless maximal cavity sizes, different dimensionless distances between the two cavities and those between the wall and the two cavities, and different values of Weber number. It is found that surface tension effects will resist the deformation of a cavity and make it closer to spherical during its growth phase, and make it collapse faster. For the case where the lower cavity is much smaller than the upper one, when the Weber number is less than or equal to 20, during the collapse phase, surface tension will have substantial effects on the behavior of the lower cavity such as change the form or the direction of its liquid jet if the Bjerknes forces to the lower cavity induced by the wall and the upper one are nearly equal. In all of the other cases, when the Weber number is greater than or equal to 10, surface tension will not have qualitative effects on the behavior of the cavity but change the length, width or sizes of its liquid jet. It is also found that for a convex cavity, surface tension has the effects on cavity behavior similar to those of the difference between the ambient pressure and the saturated vapor pressure inside the cavities. The above phenomena induced by surface tension effects are explained by this mechanism.

DOI: 10.1103/PhysRevE.71.066302 PACS number(s): 47.55.Bx, 47.55.Dz

I. INTRODUCTION

Cavitation damages occurring in structures of hydraulic machines such as ship propellers, turbine blades and valves are closely associated with the collapse of cavities near a solid wall. Theoretical study of the problem is difficult due to large deformation of the cavities. It has been investigated primarily by experimental and numerical means. In numerical simulation of the problem, the incompressible liquid flow induced by the transient cavities can be assumed inviscid and irrotational because of the high Reynolds number of the flow and the adaptive deformation of the cavities. Therefore boundary integral method is one of the most efficient methods in the numerical simulation of the problem. By this method, Ref. [1] investigated the growth and collapse of a transient cavity near a rigid wall in the presence of buoyancy force and incident stagnation-point flow, Ref. [2] studied the growth, collapse and rebound of a transient cavity containing some noncondensible contents near a rigid wall. The method was developed by Refs. [3,4] to allow a continuous simulation of growth, collapse, jet impact and penetration of a cavity near a rigid wall. Because bubbles often occur in large numbers, it is important to understand the mechanism of bubble interactions as well as their response to ambient flow field and nearby boundaries. References [5,6] studied experimentally and numerically the growth and collapse of two cavitation bubbles near a rigid wall with the buoyancy force being neglected.

In all of the above mentioned works the flow was assumed to be axisymmetric and surface tension effects were neglected. However, in some cases such as the case where the cavities are small, or more importantly, as pointed out by Ref. [1], where the cavities collapse under small difference between the ambient pressure and the saturated vapor pressure inside the bubbles (for example, the liquid cavities near the surfaces of spacecraft parts working in a microgravity condition), surface tension effects can be important. On a study of underwater explosion, Ref. [7] states on p. 1054 that "…surface tension has only a very small influence compared to calculations without surface tension. The results obtained are almost indistinguishable." By noting that according to the data provided by Ref. [7] and by taking 0.07 N/m as the value of surface tension between water and gas, the Weber number of the problem simulated by Ref. [7] is 8.56×10^7, very much higher than that in the cavitation bubble problems, it is obvious that as to surface tension effects, the situation in Ref. [7] is totally different from ours. Reference [8] studied numerically surface tension effects on the behavior of a cavity near a rigid wall. The purpose of this paper is, by boundary integral method, to investigate numerically the surface tension effects on the behavior of two cavities growing and collapsing axisymmetrically near a rigid wall.

II. GOVERNING EQUATIONS AND NUMERICAL METHODS

Suppose an infinite and initially stationary liquid with density ρ is above a rigid plane $z=0$. Initially, within the liquid there are two small spherical cavities S_1 and S_2 near the rigid wall with their centers line at the z axis. In this paper S_1 always denotes the larger bubble. The initial radii of S_1 and S_2 are R_{01} and R_{02}, and the initial distances of their centers to the wall are z_{01} and z_{02}, respectively. Therefore the liquid flow in the region D induced by the subsequent growth and collapse of the bubbles will be axisymmetric, where D is above the rigid wall $z=0$ and outside the bubbles. In this

*Email address: zhangzhenyu@fudan.edu.cn.
†Corresponding author. Email address: hszhang@fudan.edu.cn.

paper, it is assumed that the ambient pressure p_∞ and the saturated vapor pressure p_c inside the bubbles are constants and the effects of buoyancy force are neglected because usually the cavities are small and the lifetime associated with their growth and collapse is very short. The incompressibility and the irrotationality of the liquid flow leads to that the flow velocity $\mathbf{u}=\nabla\phi$ and the potential ϕ satisfies Laplace equation, $\nabla^2\phi=0$. Application of Green's theorem leads to the boundary integral formulation of the problem,

$$\sum_{k=1}^{2}\int\int_{S_k}\left[G(\mathbf{x},\mathbf{y})\frac{\partial\phi(\mathbf{y})}{\partial\mathbf{n}}-\phi(\mathbf{y})\frac{\partial G(\mathbf{x},\mathbf{y})}{\partial\mathbf{n}}\right]ds(\mathbf{y}) = 4\pi\phi(\mathbf{x}),\quad \mathbf{x}\in D, \tag{1}$$

$$\int\int_{S_k}\left\{G(\mathbf{x},\mathbf{y})\frac{\partial\phi(\mathbf{y})}{\partial\mathbf{n}}-[\phi(\mathbf{y})-\phi(\mathbf{x})]\frac{\partial G(\mathbf{x},\mathbf{y})}{\partial\mathbf{n}}\right\}ds(\mathbf{y}) + \int\int_{S_{3-k}}\left[G(\mathbf{x},\mathbf{y})\frac{\partial\phi(\mathbf{y})}{\partial\mathbf{n}}-\phi(\mathbf{y})\frac{\partial G(\mathbf{x},\mathbf{y})}{\partial\mathbf{n}}\right]ds(\mathbf{y}) = 4\pi\phi(\mathbf{x}),\quad \mathbf{x}\in S_k,\quad k=1,2. \tag{2}$$

In the above surface integrals $\mathbf{n}$ is the inward unit normal of a bubble and $G(\mathbf{x},\mathbf{y})$ is the Green's function defined by

$$G(\mathbf{x},\mathbf{y})=\frac{1}{|\mathbf{x}-\mathbf{y}|}+\frac{1}{|\tilde{\mathbf{x}}-\mathbf{y}|},$$

where $\tilde{\mathbf{x}}$ is the reflection of the position vector $\mathbf{x}$ relative to the plane $z=0$. The Bernoulli's equation is

$$\frac{\partial\phi}{\partial t}+\frac{1}{2}u^2+\frac{p}{\rho}=\frac{p_\infty}{\rho},\quad \mathbf{x}\in D, \tag{3}$$

where $u=|\mathbf{u}|$. The application of the dynamical boundary condition

$$p_s-p_c=\sigma\nabla\cdot\mathbf{n},\quad \mathbf{x}\in S_1\cup S_2$$

to the Bernoulli's equation on the bubble surfaces yields

$$\frac{\partial\phi}{\partial t}+\frac{1}{2}u^2=\frac{\Delta p}{\rho}-\frac{\sigma}{\rho}\nabla\cdot\mathbf{n},\quad \mathbf{x}\in S_1\cup S_2, \tag{4}$$

where p_s and σ are respectively the liquid pressure and surface tension on the bubble surfaces, and $\Delta p=p_\infty-p_c$. By introducing the following dimensionless quantities

$$\hat{\mathbf{x}}=\frac{\mathbf{x}}{R_{1m}},\quad \hat{t}=\frac{t\sqrt{\Delta p/\rho}}{R_{1m}},\quad \hat{\mathbf{u}}=\mathbf{u}\sqrt{\rho/\Delta p},$$

$$\hat{\phi}=\frac{\phi\sqrt{\rho/\Delta p}}{R_{1m}},\quad \hat{p}=\frac{p-p_c}{\Delta p},$$

$$\hat{R}_{1m}=1,\quad \hat{R}_{2m}=\frac{R_{2m}}{R_{1m}},\quad \hat{R}_{01}=\frac{R_{01}}{R_{1m}},\quad \hat{R}_{02}=\frac{R_{02}}{R_{1m}},$$

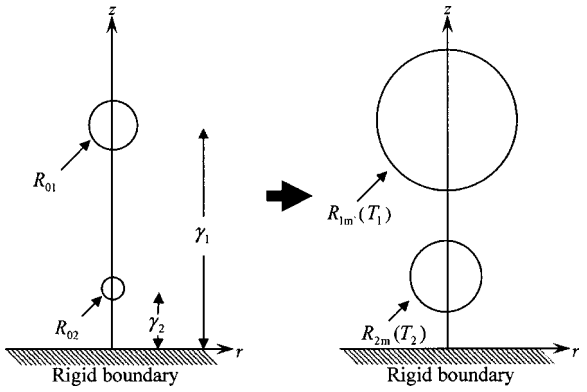

FIG. 1. The dimensionless schematic sketch of the axisymmetric geometry used in the consideration of two bubbles interaction near a rigid wall.

$$\gamma_1=\frac{z_{01}}{R_{1m}},\quad \gamma_2=\frac{z_{02}}{R_{1m}},$$

and dropping the notation " ^ " over all of the dimensionless quantities, the dimensionless form of Eqs. (1) and (2) are kept unchanged and the dimensionless forms of Eqs. (3) and (4) are respectively

$$\frac{\partial\phi}{\partial t}+\frac{1}{2}u^2+p=1,\quad \mathbf{x}\in D, \tag{5}$$

$$\frac{d\phi}{dt}\equiv\frac{\partial\phi}{\partial t}+\mathbf{u}\cdot\nabla\phi=1+\frac{1}{2}u^2-\beta\nabla\cdot\mathbf{n},\quad \mathbf{x}\in S_1\cup S_2, \tag{6}$$

where R_{1m} and R_{2m} are respectively the maximal equivalence radii of the two bubbles, and the dimensionless parameter β is the reciprocal of the Weber number and is defined by

$$\beta=\frac{\sigma}{R_{1m}\Delta p}.$$

The value of β is a measure of the relative importance between the pressure difference Δp and σ/R_{1m}, the pressure induced by the surface tension effects. When β is very small, surface tension effects can be neglected; when β is large, surface tension effects will be important. For a spherical cavity in water with 1 mm maximal equivalence diameter collapsing at pressure difference $\Delta p=1000P_a$ and at temperature 10 °C, the value of β is about 0.15. Figure 1 gives the dimensionless schematic sketch of the axisymmetric geometry used in the consideration of two bubbles interaction near a rigid wall, where the abscissa and ordinate are respectively the radially and axially cylindrical coordinates.

The way of solution is as follows. Suppose at time t we have known the bubble shapes and the potential ϕ on the bubbles. Then at this time the tangential and normal velocities on the bubbles can be obtained by calculating the tangential gradient of ϕ on the bubbles and solving the system of integral equations (2) for $\partial\phi/\partial n$ on the bubbles respec-

tively. Thus we can obtain the velocity **u** of the bubble surface. The bubble shapes at time $t+\Delta t$ can be obtained by time integration of the equation

$$\frac{d\mathbf{x}}{dt} = \mathbf{u}, \quad \mathbf{x} \in S_1 \cup S_2. \tag{7}$$

At time $t+\Delta t$ the potential ϕ on the bubbles can be obtained by time integration of Eq. (6). At any time t if ϕ and $\partial\phi/\partial n$ on the bubbles have been known, then the potential ϕ and thus **u**, and the pressure p in D at this time can in turn be obtained by evaluation of the integral on the left-hand side of Eqs. (1) and by use of Bernoulli's equation (5). As the problem is axisymmetric the Green's function can be integrated in the azimuthal direction, which reduces Eq. (2) into a system of integral equations on the semi-meridian-lines of the bubbles. The integrands of the reduced integral equations contain some complete elliptic integrals of first and third kinds. Note that this kind of expression for Eq. (2) has the advantage that in the reduced integral equations the function corresponding to the second term in the integrand of the first integral of Eq. (2) are smooth. The singularity contained in the complete elliptic integrals can be removed by subtracting a proper logarithm function. Thus the integrands of the reduced integral equations only contain smooth functions and productions of a logarithm function and smooth functions.

To solve the problem numerically, any of the semimeridian lines is divided into N elements. In this paper we take $N=32$. Integral on any of the semimeridian lines is reduced to the sum of integrals on the N elements. Within any elements, ϕ, $\partial\phi/\partial n$ and the arc shape are approximated by linear interpolations based on their values at the end points of the element. On any element the integral of smooth functions and that of functions containing logarithmic singularity are integrated numerically by four point Gauss-Legendre quadrature and four points Gaussian quadrature with singular logarithm function as its weight respectively [9]. In order to avoid numerical integration of a smooth function with large gradient, on any element which does not contain any singularity point but is near a singularity point, the integral is pre-treated by several times of integration by parts before it is integrated numerically. Spatial derivatives of unknown functions appeared in the integrals or in the partial differential equations are approximated by second order centered differences. Thus the integral equations are reduced to a system of linear algebraic equations with the nodal point values of $\partial\phi/\partial n$ as the unknowns, and the partial differential equations (6) and (7) are reduced to a system of ordinary differential equations with the corresponding nodal values as the unknown functions. In this paper the system of linear algebraic equations is solved by Gaussian elimination method with partial pivot. The numerical method suffers the Courant-Frederic-Levy (CFL) type instability induced by high fluid velocity and the dissipative type instability induced by the surface tension terms so that the maximal allowed time step Δt is much smaller than the grid spacing. Therefore, even if a low order scheme is used to solve the system of ordinary differential equations, the accuracy in time integration can also be ensured. In this paper the system of ordinary differential equations is solved by Eulerian method. At any time t, the time step Δt is dynamically taken to be

$$\Delta t = \frac{\Delta t_0}{1 + \frac{1}{2}u_{\max}^2},$$

where $u_{\max}$ is the maximal bubble velocity at time t and Δt_0 is the initial time step. In calculations, the larger the value of β is, the smaller of the value of Δt_0 should be taken. For example, in the case of $\gamma_1=3$, $\gamma_2=0.5$, $R_{1m}=1$, $R_{2m}=0.5$, $R_{01}=0.2$, and $R_{02}=0.1$, the initial time step Δt_0 are 0.01, 0.005, and 0.0025, respectively, for $\beta=0$, 0.05, and 0.1. In order to avoid nonlinear numerical instability induced by the accumulations of markers on the bubble surface, it is necessary to use grid reconstruction techniques. The grid reconstruction techniques based on usual interpolation of high order polynomials or splines will cause unwanted numerical oscillations. To suppress the numerical oscillations, it is necessary to employ some artificial smoothing techniques without any physical meaning. In this paper the used grid reconstruction method is based on the ENO interpolation of third order polynomials [10], which can remove the numerical oscillations without employment of any artificial smoothing technique.

It is found in the numerical simulations that if the initial value of the potential ϕ on the bubbles is taken to be the Rayleigh bubble solutions,

$$\phi_{0k} = -R_{0k}\sqrt{\frac{2}{3}\left[\left(\frac{R_{km}}{R_{0k}}\right)^3 - 1\right] + \frac{2\beta}{R_{0k}}\left[\left(\frac{R_{km}}{R_{0k}}\right)^2 - 1\right]}, \quad \text{on } S_k, \quad k=1,2, \tag{8}$$

the computed maximal equivalence radii will be far away from their preassigned values $R_{km}(k=1,2)$. This difficulty has been overcome by Newton-Raphson iterations for $\phi_{0k}(k=1,2)$ with the Rayleigh bubble solutions (8) only as the initial values of the iterations [5]. In this paper we take $R_{01}=0.2$ and $R_{02}=R_{01}\cdot R_{2m}$. The partial derivatives in the Jacobian matrix appeared in Newton-Raphson iterations are approximated by finite differences. In three iterations the relative error of the maximal bubble volumes is always less than 0.001, i.e., the relative error of the maximal equivalence radii is less than about 0.0003.

III. NUMERICAL RESULTS

A. The mechanism of surface tension effects

Before we analyze the mechanism of surface tension effects, let us analyze first the mechanism of the effects of pressure difference $\Delta p=p_\infty-p_c$ on an experimentally spark- or laser-generated cavity growing and collapsing spherically in an initially stationary liquid under this pressure difference. The effects of the pressure difference have the tendency to reduce the volume of the cavity. Therefore, during the growth phase, the pressure difference has the effects to resist the deformation of the cavity and thus to stabilize the physical process, whereas during the collapse phase, it has the effects to accelerate the deformation of the cavity and thus to

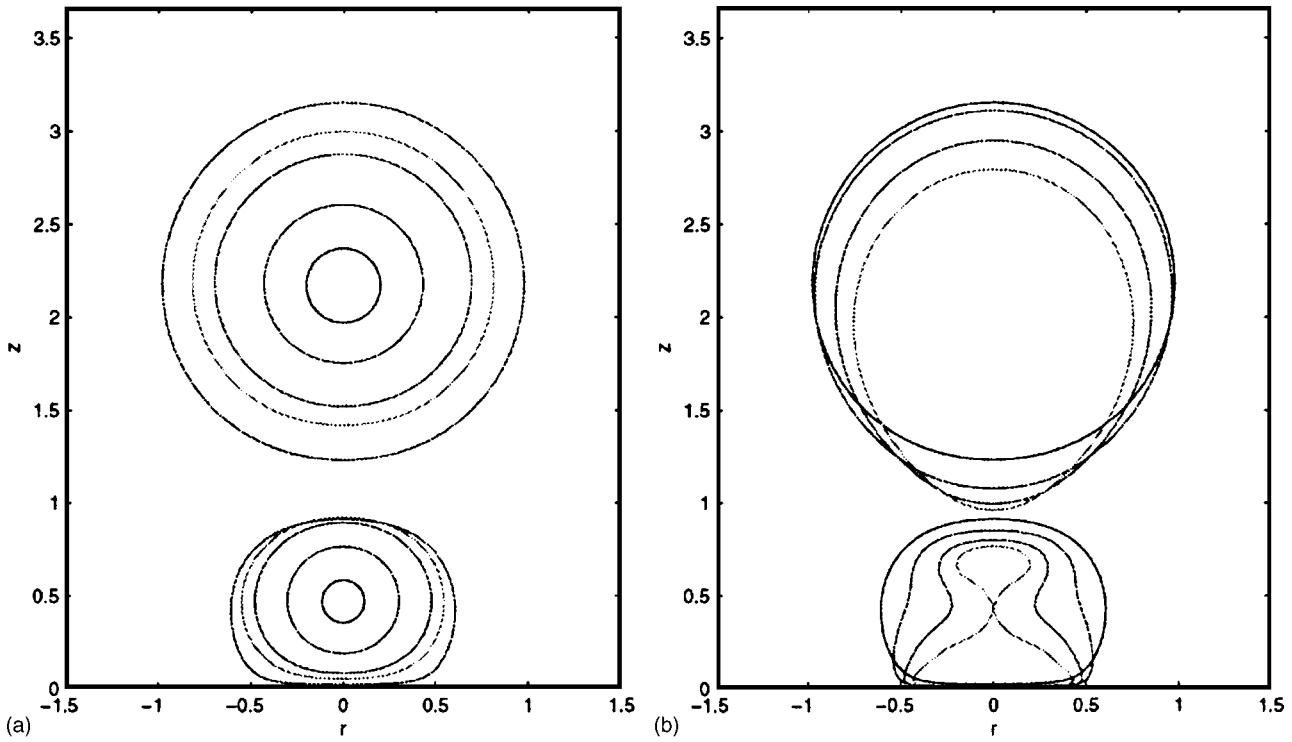

FIG. 2. (Color online) Bubble profiles for $R_{1m}=1$, $R_{2m}=0.57$, $\gamma_1=2.17$, $\gamma_2=0.47$, $\beta=0$, $R_{01}=0.1$, and $R_{02}=0.057$. (a) The growth phase; (b) the collapse phase. This is the same case of Fig. 6(a) and Fig. 10(a) in Ref. [5].

destabilize the physical process. When a cavity is near a boundary (a rigid wall, another cavity or a free surface), under a pressure difference, it will basically keep spherical shapes during its growth phase, and will be far away from the spherical shape during its collapse phase, due to the stabilizing and destabilizing effects of the pressure difference on the two physical processes, respectively. Due to the resistance of the wall, to the change of the width of the flow channel between the cavity and the wall, when a cavity grows near a rigid wall its centroid will move away from the wall, and when a cavity collapses near a rigid wall, its centroid will move approaching to the wall. The approaching movement of the cavity centroid to the wall will cause the liquid to flow around the cavity from its near wall side to its opposite side, causing the flow blocked near its further side from the wall, the increase of the liquid pressure, and large pressure gradient there, which will induce a wall directed liquid jet to form and to develop there and produce a wall directed resultant force to the cavity, called Bjerknes force induced by the wall.

For two neighboring cavities which are initially spherical, also due to the resistance of the bubbles to the change of the width of the flow channel between the two bubbles, during the growth phase their centroids will move away from each other, and during the collapse phase their centroids will move approaching to each other so that the flows around the two cavities will be from their near sides to their far sides, causing the flow blocked near their far sides, the increase of the liquid pressure, and the large pressure gradient there, and producing a resultant force to any of the cavities, which is

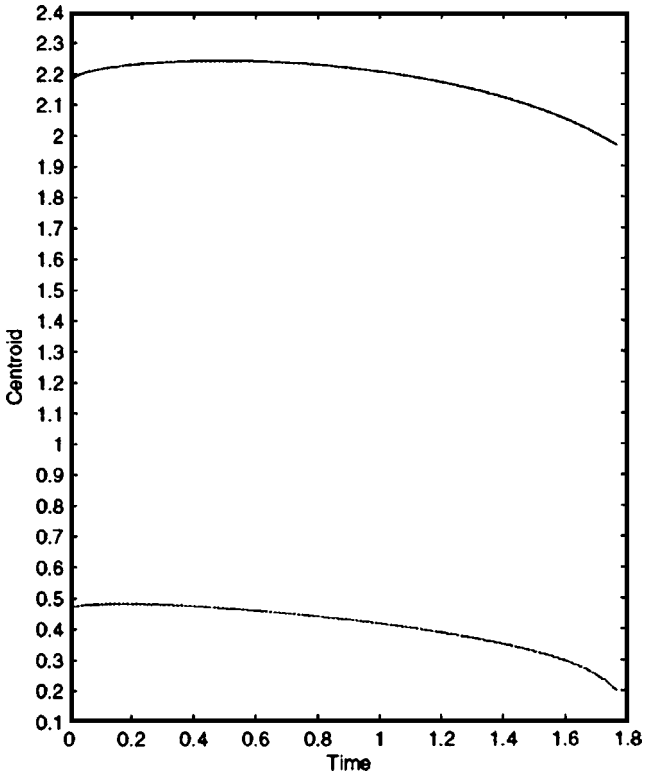

FIG. 3. (Color online) Centroid positions of the bubbles corresponding to the case of Fig. 2.

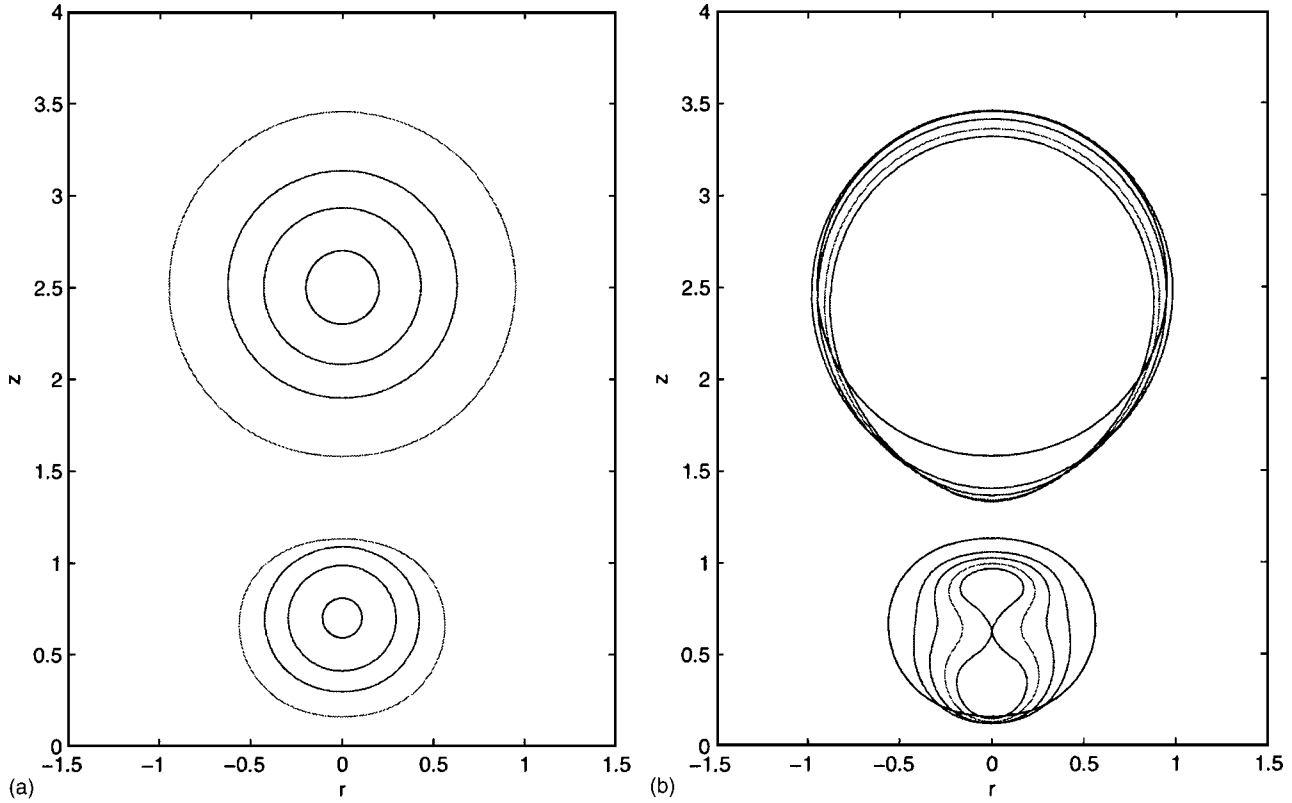

FIG. 4. (Color online) Bubble profiles for $R_{1m}=1$, $R_{2m}=0.54$, $\gamma_1=2.5$, $\gamma_2=0.7$, $\beta=0$, $R_{01}=0.1$, and $R_{02}=0.054$. (a) The growth phase; (b) the collapse phase. This is the same case of Fig. 7(a)-1 and Fig. 7(b)-1 in Ref. [6].

directed to the other cavity, called Bjerknes force to the cavity induced by the other cavity. If there appears any liquid jet during the collapse phase of one cavity, the jet must be directed to the other cavity. By noting that the response of a larger cavity to an action will be smaller than that of a smaller cavity to an action of same size due to its bigger inertia, the smaller cavity will collapse faster than the larger one.

For two cavities growing and collapsing axisymmetrically near a rigid wall, their behavior will depend on their sizes, the distance between the two cavities, and the distances between the wall and the two cavities. For example, during the collapse phase, in all cases the centroid of the upper cavity must move to the wall, and the liquid jet, if it appears, must be directed to the wall because the Bjerknes forces induced by the lower cavity and the wall to the upper cavity are both directed to the wall. The Bjerknes forces induced by the upper cavity and the wall to the lower cavity are in opposite directions. Therefore when a small cavity is located between a large cavity and a rigid wall, during the collapse phases, its centroid must move to the wall and its liquid jet must be directed to the wall if it is near the wall and far away from the large cavity; its centroid must move away from the wall and its liquid jet must be directed away from the wall if it is near the large cavity and far away from the wall; and it will be elongated in vertical direction and its liquid jet will be annular if the Bjerknes forces to it induced by the large cavity and the wall are nearly equal.

Because for a convex cavity, surface tension has the effect to reduce the area of its surface and thus reduce its volume and generate an inward pressure on its surface, which is similar to that of the pressure difference, surface tension also has the stabilizing and destabilizing effects on the deformation of a cavity during its growth and collapse phases, respectively. By this mechanism in some cases it will not be difficult to analyze surface tension effects on cavity behavior. For example, during the growth phase surface tension will make a cavity closer to spherical shape. It will accelerate the collapse of a cavity. For a cavity near a rigid wall, during its collapse phase, surface tension effects will make its centroid move more to the wall and make its downward liquid jet wider. For two neighboring cavities in an infinite liquid, during their collapse phase, surface tension will make their centroids move closer and make the liquid jet of the smaller bubble wider.

Now we analyze the mechanism of surface tension effects on the behavior of two cavities growing and collapsing axisymmetrically near a rigid wall. First we consider the case where R_{2m} is much smaller than R_{1m} and the upper cavity is the smaller one. During the collapse phase, the Bjerknes forces to the upper cavity induced by the wall and the lower cavity are in same direction (downward), whereas the Bjerknes forces to the lower cavity induced by the wall and the upper one are in opposite direction. Therefore the resultant force of the former will be larger than that of the latter. By noting that the inertia of the upper (smaller) cavity is much smaller than that of the lower (larger) cavity and that the action of surface tension to the upper cavity is much smaller than the resultant force of the Bjerknes forces to it, the upper cavity will collapse much faster than the lower one

TABLE I. The dynamic scenarios of the cavity during the collapse phase (annular: an annular jet; ↑: upwards; ↓: downwards; —: the width of the jet is incomparable).

Case			Jet direction	Jet width or size	Centroid motion during the later time of the collapse phase	Period of the collapse phase
	$R_{1m}=1$, $R_{2m}=0.5$	$\beta=0$	annular	—	↓	0.814
case 1	$\gamma_1=2.25$, $\gamma_2=0.5$	$\beta=0.05$	↓	thinner	↓	0.655
	lower cavity	$\beta=0.1$	↓	wider	↓	0.575
	$R_{1m}=1$, $R_{2m}=0.5$	$\beta=0$	↑	thin	↑	0.723
case 2	$\gamma_1=2.75$, $\gamma_2=1$	$\beta=0.05$	annular	—	↑	0.597
	low cavity	$\beta=0.1$	↓	thin	↓	0.529
	$R_{1m}=1$, $R_{2m}=0.5$	$\beta=0$	↓	thinnest	↓	0.711
case 3	$\gamma_1=3$, $\gamma_2=0.5$	$\beta=0.05$	↓	wider	↓	0.627
	lower cavity	$\beta=0.1$	↓	widest	↓	0.564
	$R_{1m}=1$, $R_{2m}=0.5$	$\beta=0$	↑	widest	↑	0.683
case 4	$\gamma_1=3.25$, $\gamma_2=1.5$	$\beta=0.05$	↑	thinner	↑	0.556
	lower cavity	$\beta=0.1$	↑	thinner	↑	0.490
	$R_{1m}=1$, $R_{2m}=1$	$\beta=0$	↓	thinner	↓	1.111
case 5	$\gamma_1=5.25$, $\gamma_2=3$	$\beta=0.05$	↓	wider	↓	1.076
	upper cavity	$\beta=0.1$	↓	widest	↓	1.041
	$R_{1m}=1$, $R_{2m}=1$	$\beta=0$	↓	thinner	↓	1.121
case 6	$\gamma_1=3.5$, $\gamma_2=1$	$\beta=0.05$	↓	wider	↓	1.074
	upper cavity	$\beta=0.1$	↓	widest	↓	0.933
	$R_{1m}=1$, $R_{2m}=0.5$	$\beta=0$	↓	larger	↓	0.561
case 7	$\gamma_1=1$, $\gamma_2=3.5$	$\beta=0.05$	↓	smaller	↓	0.498
	upper cavity	$\beta=0.1$	↓	smallest	↓	0.452
	$R_{1m}=1$, $R_{2m}=0.5$	$\beta=0$	↓	larger	↓	0.586
case 8	$\gamma_1=2$, $\gamma_2=3.75$	$\beta=0.05$	↓	smaller	↓	0.531
	upper cavity	$\beta=0.1$	↓	smallest	↓	0.468

and surface tension will not have qualitative effect but make the centroid of the upper cavity move downwards more and its downward liquid jet smaller. In this case surface tension will not have significant effects on the behavior of the lower cavity before the liquid jet of the upper cavity hits its opposite side, because during this period the lower cavity only has a very small deformation from the large spherical shape and thus its curvature is small everywhere.

Next we consider the case where R_{2m} is nearly equal to R_{1m}. Although in this case the inertias of the two cavities are nearly equal, the upper cavity will collapse faster than the lower one because the resultant force of the two Bjerknes force to the upper cavity induced by the wall and the lower cavity is larger than that of the two Bjerknes forces to the lower cavity induced by the wall and upper cavity. Therefore during the collapse phase surface tension will not have qualitative effects on the behavior of the upper cavity but make the centroid of the upper cavity move downwards more and make its downward liquid jet wider. When the two cavities are close to each other and far away from the wall, during the collapse phase, surface tension effects will make the centroid of the lower cavity move upwards more and its upward liquid jet develop more before the downward liquid jet of the upper cavity hits its lower side. When the lower cavity is near the wall and far away from the upper one, during the collapse phase, no liquid jet of the lower cavity will appear and surface tension will make the lower cavity elongated more in vertical direction before the jet impact of the upper cavity happens.

Finally we consider the case where R_{2m} is much smaller than R_{1m} and the lower cavity is the smaller one. Because of the infinite inertia of the rigid wall and the deformability of the upper cavity, in this case, it will be easier to change the width of the flow channel between the two cavities than to change the width of the flow channel between the lower cavity and the wall. Therefore, during the collapse phase, surface tension effects will have the tendency to help the centroid of the lower cavity move downwards and resist it to move upwards, and thus have the tendency to strengthen the Bjerknes force to the lower cavity induced by the wall and

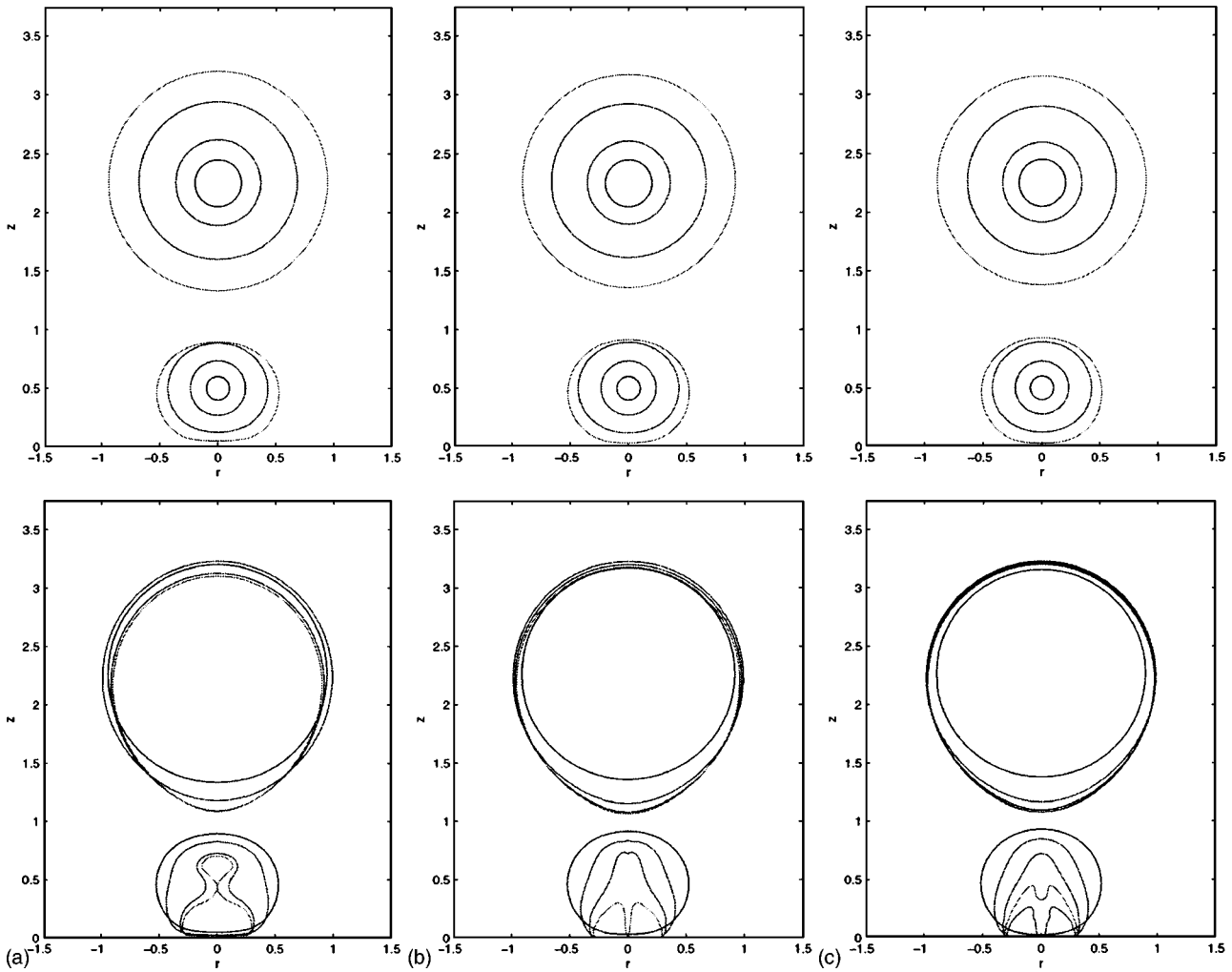

FIG. 5. (Color online) Bubble profiles for $R_{1m}=1$, $R_{2m}=0.5$, $\gamma_1=2.25$, $\gamma_2=0.5$, $R_{01}=0.2$, and $R_{02}=0.1$ during the growth phase (upper diagrams) and collapse phase (lower diagrams). (a) $\beta=0$, (b) $\beta=0.05$, and (c) $\beta=0.1$. Upper diagrams (from innermost to outermost): (a) $t=0,0.036,0.226,0.666$; (b) $t=0,0.031,0.201,0.566$; (c) $t=0,0.025,0.171,0.503$. Lower diagrams (from outermost to innermost): (a) $t=0.666,1.096,1.437,1.480$; (b) $t=0.566,0.984,1.147,1.221$; (c) $t=0.503,0.866,0.991,1.041,1.078$.

weaken the Bjerknes force to it induced by the upper cavity. The lower cavity will collapse much faster than the upper one due to its much smaller inertia. During the collapse phase, the centroid of the upper cavity will move downwards, and due to its large inertia, the upper cavity will only have a small change from the spherical shape before the jet impact of the lower cavity happens. Therefore, surface tension will not have significant effect on the upper cavity but makes its centroid move downwards more and makes it elongated more in vertical direction. If the lower cavity is near to the wall and far away from the upper cavity, during the collapse phase, surface tension effects will make its centroid move downwards more and its downward liquid jet wider. If the lower cavity is near to the upper one and far away from the wall, during the collapse phase, surface tension will make its centroid move upwards less and make its upward liquid jet thinner. If the lower cavity is near to the wall and the upper cavity, and the oppositely directional Bjerknes forces to the lower cavity induced by the wall and upper cavity respectively are nearly equal, the resultant force of the two Bjerknes forces will be very small. In this case, during the collapse phase, surface tension will have substantial effects on the behavior of the lower cavity such as change the form or the direction of its liquid jet.

B. Numerical results

In our dimensionless variables the maximal equivalence radius of the larger bubble is always $R_{1m}=1$. For $R_{1m}=1$, $R_{2m}=0.57$, $\gamma_1=2.17$, $\gamma_2=0.47$, $R_{01}=0.1$, $R_{02}=0.057$, and $\beta=0$, Fig. 2 and Fig. 3 give respectively the computed bubble profiles and the centroid positions of the bubbles during both growth and collapse phases. The results are almost exactly the same as the numerical results shown in Fig. 10(a) and in good agreements with the experimental results shown in Fig. 6(a) in Ref. [5] for the same case. For $R_{1m}=1$, $R_{2m}=0.54$, $\gamma_1=2.5$, $\gamma_2=0.7$, $R_{01}=0.1$, $R_{02}=0.054$, and $\beta=0$, Fig. 4 gives the computed bubble profiles during both the growth and collapse phases. The results are almost exactly the same as the numerical results shown in Fig. 7(b)-1 and in good agreements with the experimental results shown in Fig. 7(a)-1 in Ref. [6] for the same case. So it is believable that the math-

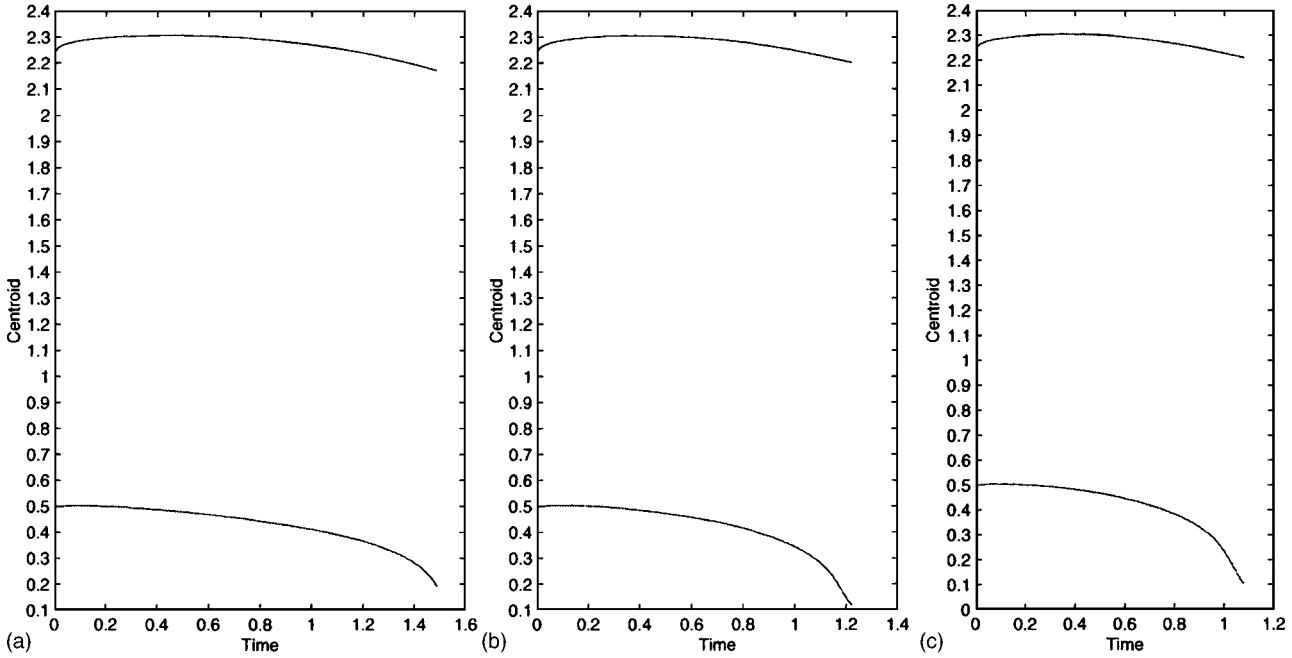

FIG. 6. (Color online) Centroid positions of the bubbles corresponding to the case of Fig. 5. (a) $\beta=0$, (b) $\beta=0.05$, and (c) $\beta=0.1$.

ematical derivation and programming of this paper are correct.

Table I gives the dynamic scenarios of the cavity during the collapse phase for different cases obtained by our numerical simulation. In cases 1–4, $R_{2m}=0.5R_{1m}$ and the lower cavity is the smaller one, which stands for the situation where the lower cavity is much smaller than the upper one. Besides, case 1 and case 2 stand for the situation where the actions to the lower cavity induced by the wall and the upper one are nearly equal; case 3 stands for the situation where the lower cavity is near the wall and far away from the upper one; and case 4 stands for the situation where the lower cavity is near the upper one and far away from the wall. In cases 5–6, $R_{2m}=R_{1m}$, which stands for the situation where the two cavities are nearly equal. Besides, case 5 stands for the situation where the lower cavity is near the upper one and far away from the wall, and case 6 stands for the situation where the lower cavity is near the wall and far away from the upper one. In cases 7–8, $R_{2m}=0.5R_{1m}$ and the upper cavity is the smaller one, which stands for the situation where the

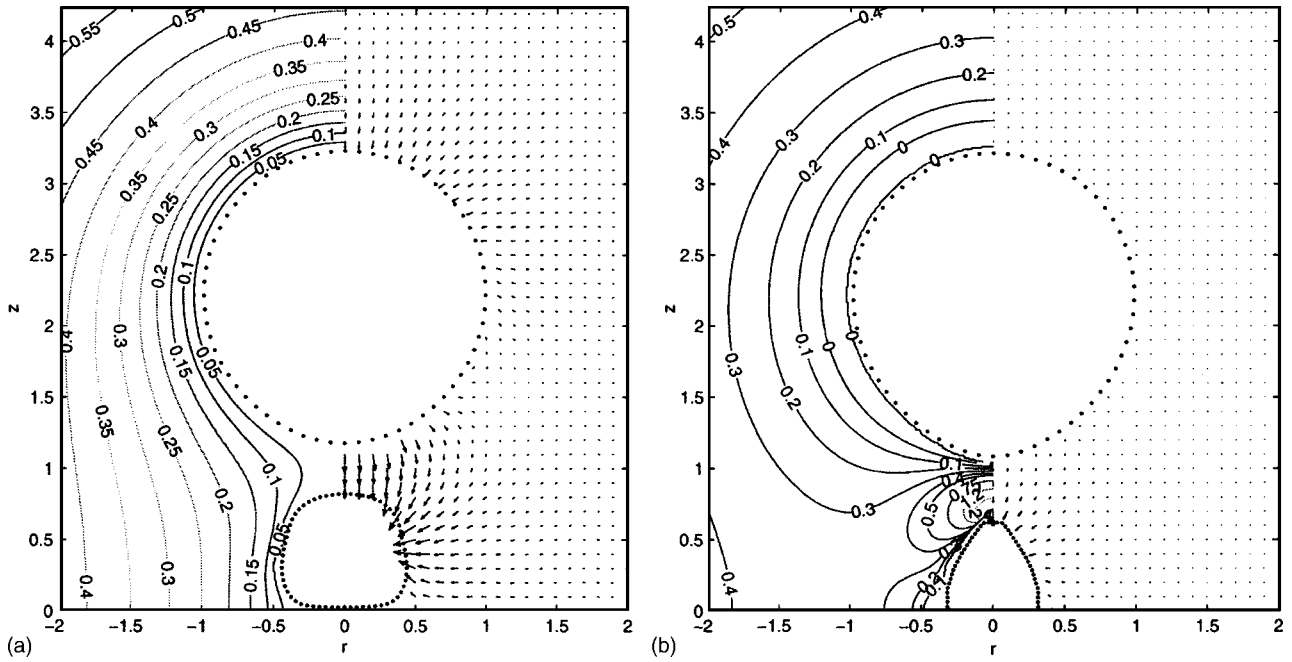

FIG. 7. (Color online) Velocity fields and pressure contours for $R_{1m}=1$, $R_{2m}=0.5$, $\gamma_1=2.25$, $\gamma_2=0.5$, $R_{01}=0.2$, and $R_{02}=0.1$. (a) $\beta=0$ and $t=1.096$; (b) $\beta=0.1$ and $t=1.010$.

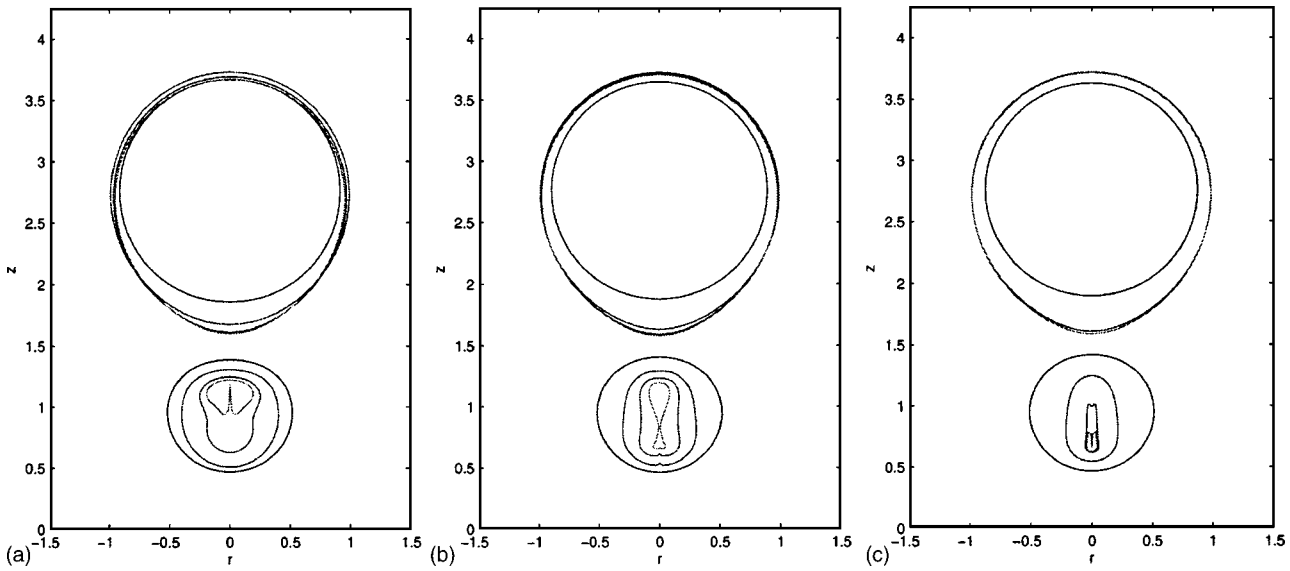

FIG. 8. (Color online) Bubble profiles for $R_{1m}=1$, $R_{2m}=0.5$, $\gamma_1=2.75$, $\gamma_2=1$, $R_{01}=0.2$, and $R_{02}=0.1$ during collapse phase. From outermost to innermost, (a) $\beta=0$, $t=0.586, 1.041, 1.248, 1.309$; (b) $\beta=0.05$, $t=0.514, 0.984, 1.075, 1.111$; (c) $\beta=0.1$, $t=0.456, 0.933, 0.983, 0.985$.

upper cavity is much smaller than the lower one. Besides, case 7 stands for the situation where the lower cavity is near the wall and far away from the upper one, and case 8 stands for the situation where the lower cavity is near the upper one and far away from the wall. It can be seen that in all cases surface tension effects make the collapse period shortened. For the case of one cavity near a rigid wall, this result was obtained by Ref. [8].

Figures 5, 8, 10, 12, 14, 16, 18, and 20 give the computed bubble profiles for cases 1–8, respectively, and Figs. 6, 9, 11, 13, 15, 17, 19, and 21 give the corresponding centroid positions of the bubbles. It can be seen from the figures that when a cavity is much smaller than the other, surface tension will not have significant effect on the behavior of the larger cavity.

Figure 5 gives the bubble profiles during both the growth and collapse phases. It can be seen from Figs. 5 and 6 that in case 1, during the growth phase the upper bubble is near spherical and its centroid moves upwards a little. The lower bubble is near spherical at the early time and then slightly shortened in vertical direction and elongated in radial direction, and its centroid moves downwards a little. During the growth phase surface tension has no significant effect on cavity shapes but makes it closer to spherical. Note that the

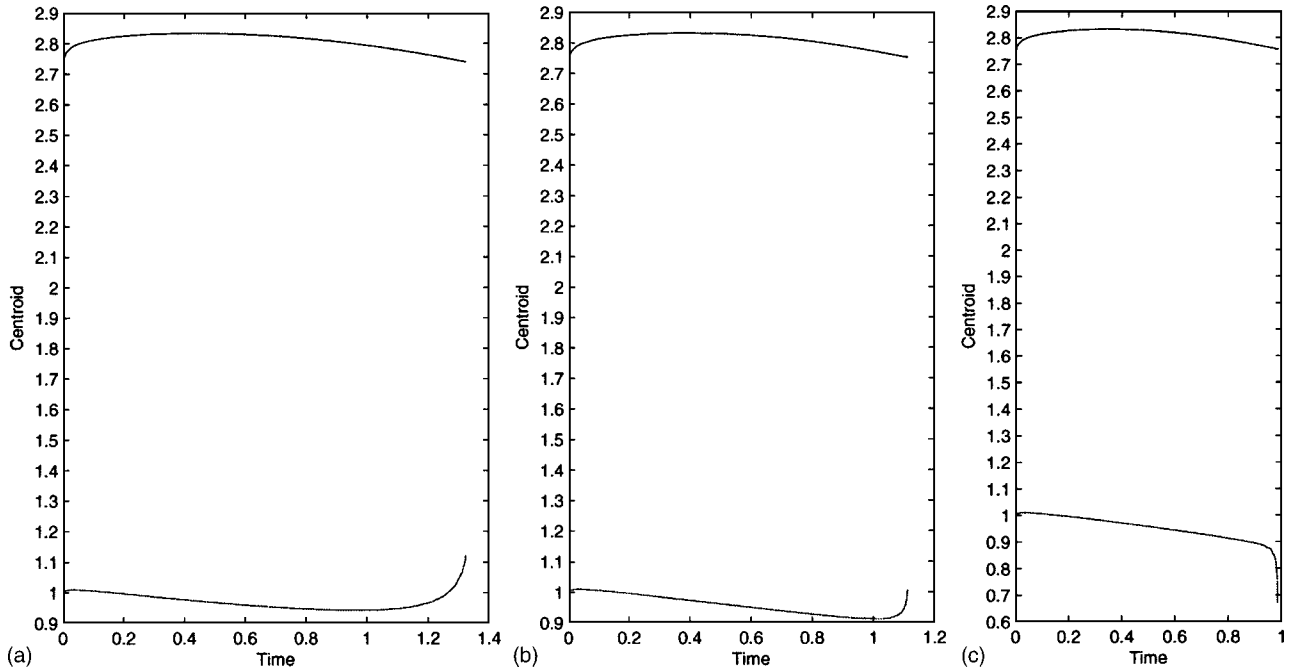

FIG. 9. (Color online) Centroid positions of the bubbles corresponding to the case of Fig. 8. (a) $\beta=0$, (b) $\beta=0.05$, and (c) $\beta=0.1$.

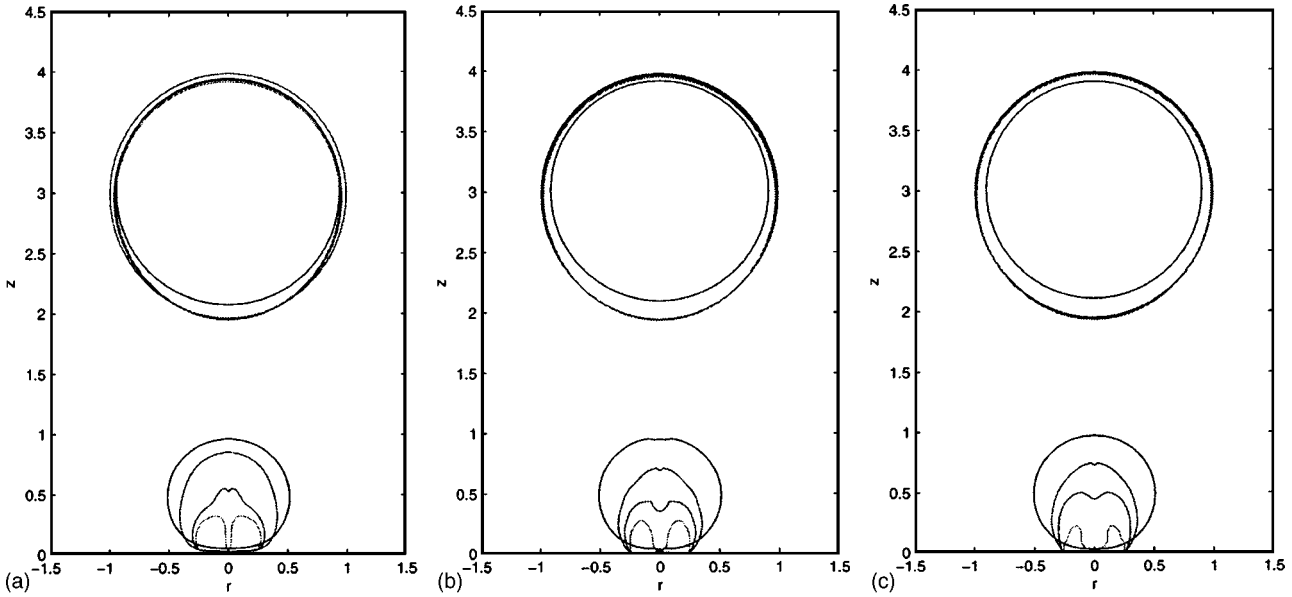

FIG. 10. (Color online) Bubble profiles for $R_{1m}=1$, $R_{2m}=0.5$, $\gamma_1=3$, $\gamma_2=0.5$, $R_{01}=0.2$, and $R_{02}=0.1$ during collapse phase. From outermost to innermost: (a) $\beta=0$, $t=0.632, 1.074, 1.299, 1.343$; (b) $\beta=0.05$, $t=0.547, 1.040, 1.121, 1.174$; (c) $\beta=0.1$, $t=0.498, 0.914, 0.985, 1.062$.

period of growth phase of the lower bubble for $\beta=0$, 0.05, and 0.1 cases, is respectively 0.666, 0.566, and 0.503, which decreases when the value of β increases. This is because in order to reach the same maximal volume the initial velocity must increase when the value of β increases (for $\beta=0$, 0.05, and 0.1 cases, the initial potential of the lower bubble is -1.3674, -1.5129, and -1.6596, respectively). If the initial potentials are taken the same value -1.3674, then during the growth phase the volume of the lower bubble for $\beta=0$, 0.05, and 0.1 cases is respectively 0.150, 0.145, and 0.140 (at $t=0.1$); 0.276, 0.260, and 0.240 (at $t=0.2$); 0.375, 0.335, and 0.296 (at $t=0.3$). Therefore it is true that surface tension

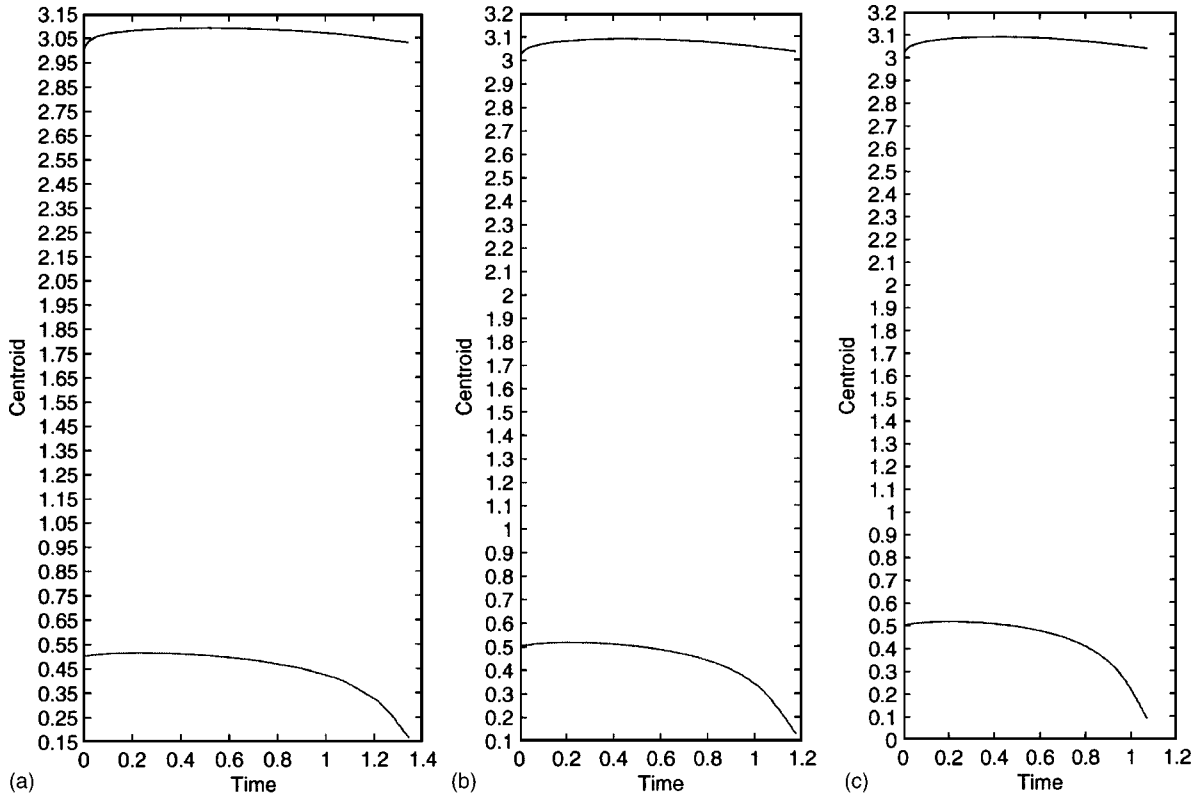

FIG. 11. (Color online) Centroid positions of the bubbles corresponding to the case of Fig. 10. (a) $\beta=0$, (b) $\beta=0.05$, and (c) $\beta=0.1$.

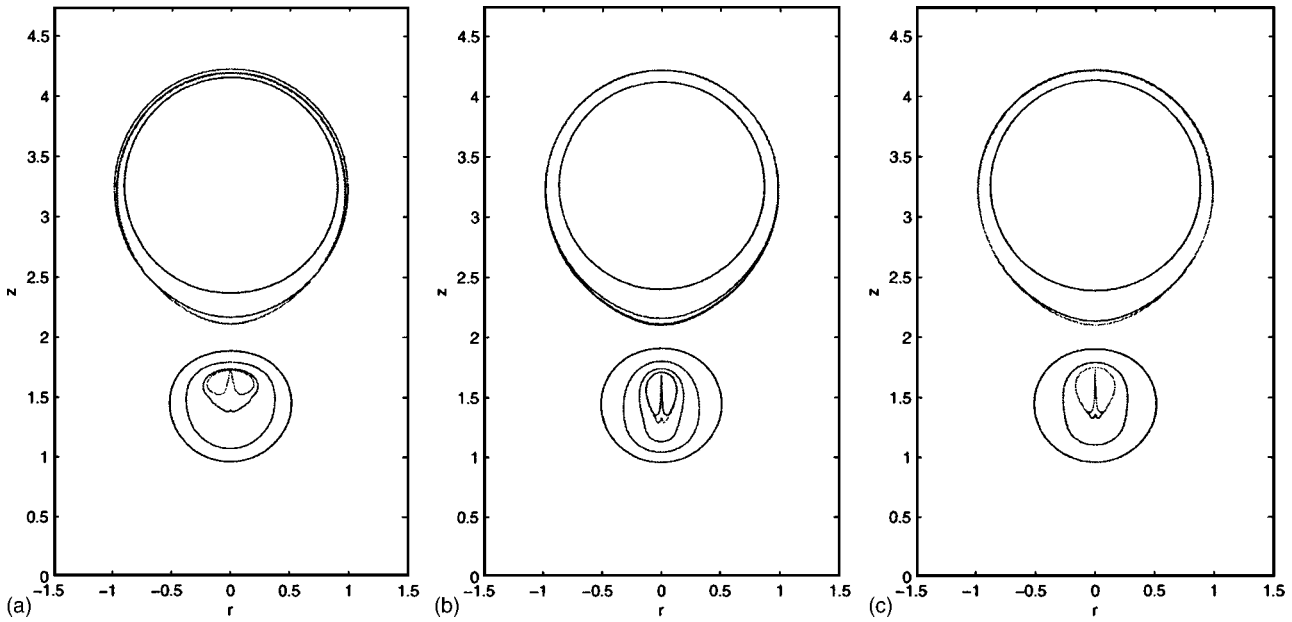

FIG. 12. (Color online) Bubble profiles for $R_{1m}=1$, $R_{2m}=0.5$, $\gamma_1=3.25$, $\gamma_2=1.5$, $R_{01}=0.2$, and $R_{02}=0.1$ during collapse phase. From outermost to innermost: (a) $\beta=0$, $t=0.556, 1.036, 1.214, 1.239$; (b) $\beta=0.05$, $t=0.484, 0.968, 1.040473, 1.040474$; (c) $\beta=0.1$, $t=0.439, 0.825, 0.906, 0.92848, 0.92896$.

effects make the growth of a cavity slower. In all of the other cases we will not give the bubble profiles in growth phase because the basic behavior are similar. In case 1, during the collapse phase, surface tension effects make the centroid of the lower cavity move downwards more and make the direction of its liquid jet change from annular ($\beta=0$ case) to downward ($\beta=0.05$ and 0.1 cases). Just before the liquid jet forms, Fig. 7 gives the computed flow fields and pressure contours for $\beta=0$ and 0.1 cases. It can be seen that when $\beta=0$, near the upper part of the flank of the lower bubble, both the velocity and the minus pressure gradient of the liquid are large and point to the bubble, which indicates that an annular liquid jet will begin to form; whereas when $\beta=0.1$, there is a pressure maximum near the top of the lower bubble and at the axisymmetric axis, and the pressure gradient and the velocity nearby are both large, which indicates that a downward liquid jet will begin to form there.

It can be seen from Figs. 8 and 9 that in case 2, during the collapse phase surface tension effects make the direction of the jet of the lower cavity change from upward ($\beta=0$ case) to

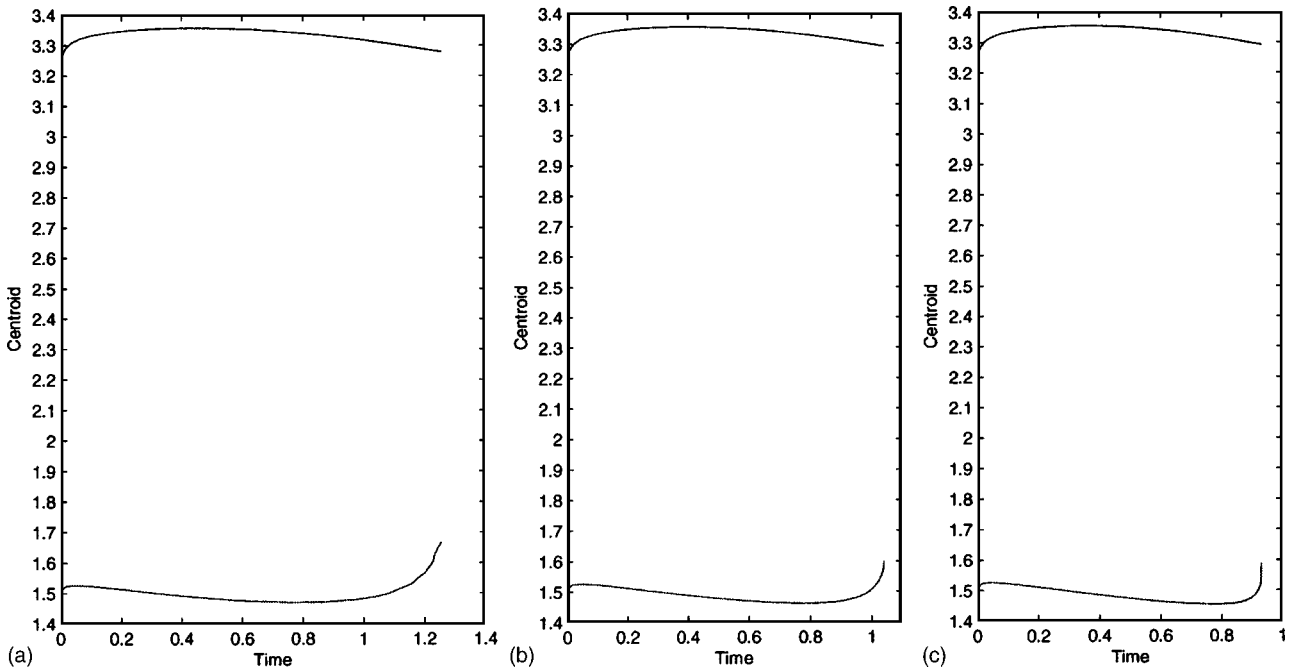

FIG. 13. (Color online) Centroid positions of the bubbles corresponding to the case of Fig. 12. (a) $\beta=0$, (b) $\beta=0.05$, and (c) $\beta=0.1$.

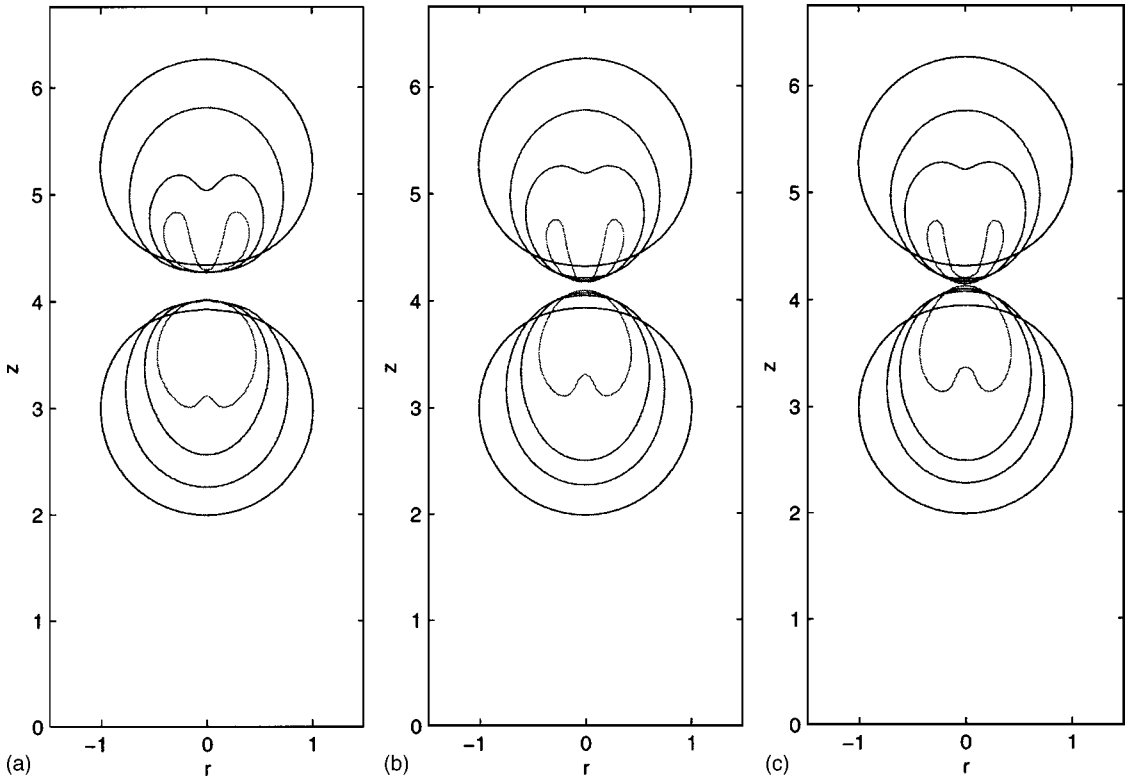

FIG. 14. (Color online) Bubble profiles for $R_{1m}=R_{2m}=1$, $\gamma_1=5.25$, $\gamma_2=3$, and $R_{01}=R_{02}=0.2$ during the collapse phase. From outermost to innermost: (a) $\beta=0$, $t=1.099, 1.899, 2.112, 2.210$; (b) $\beta=0.05$, $t=1.044, 1.828, 1.987, 2.120$; (c) $\beta=0.1$, $t=0.988, 1.754, 1.891, 2.029$.

annular ($\beta=0.05$ case) and then to downward ($\beta=0.1$ case). Note that during the collapse phase, the centroid of the lower cavity moves downwards at most of the time and moves upwards quickly at the very late time in $\beta=0$ and 0.05 cases, but it moves downwards at all of the time in $\beta=0.1$ case. Therefore in case 1 and case 2, during the collapse phase surface tension has substantial effects on the behavior of the lower cavity.

It can be seen from Figs. 10 and 11 that in case 3, during the collapse phase surface tension effects make the centroid of the lower cavity move downwards more and make its downward liquid jet wider.

It can be seen from Figs. 12 and 13 that in case 4, during the collapse phase surface tension effects make the lower cavity elongated in vertical direction, its centroid move upwards less, and its upward liquid jet thinner. Note that during the collapse phase the centroid of the lower cavity moves downwards at most of the time and upwards quickly at the very late time.

It can be seen from Figs. 14 and 15 that in case 5, the upper cavity collapses much faster than the lower one. During the collapse phase, surface tension effects make the centroid of the upper cavity move downwards more and the centroid of the lower cavity move upwards more (therefore

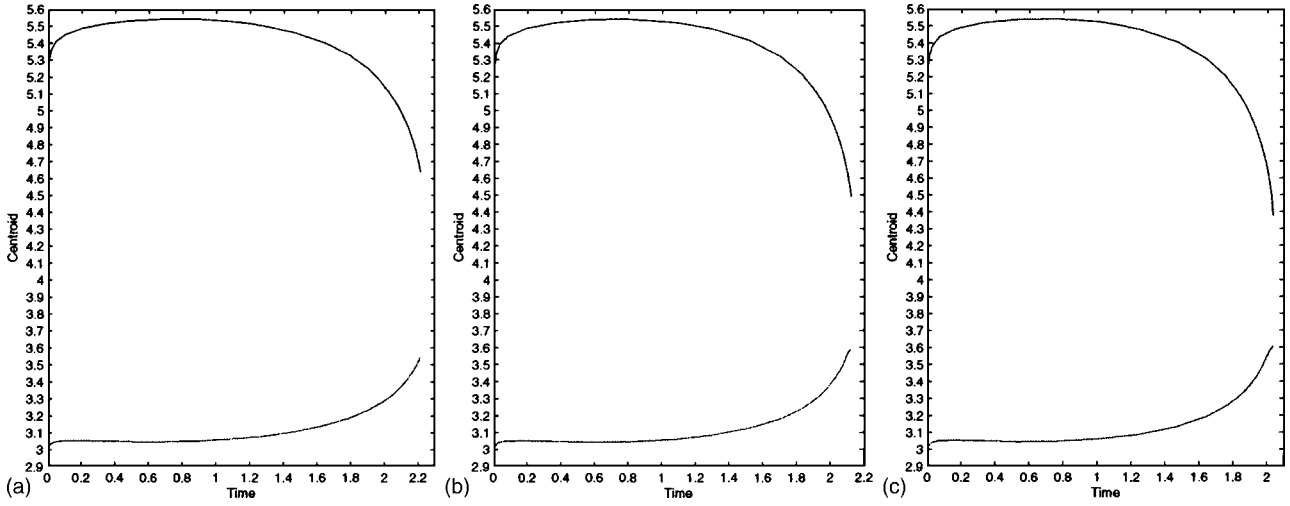

FIG. 15. (Color online) Centroid positions of the bubbles corresponding to the case of Fig. 14. (a) $\beta=0$, (b) $\beta=0.05$, and (c) $\beta=0.1$.

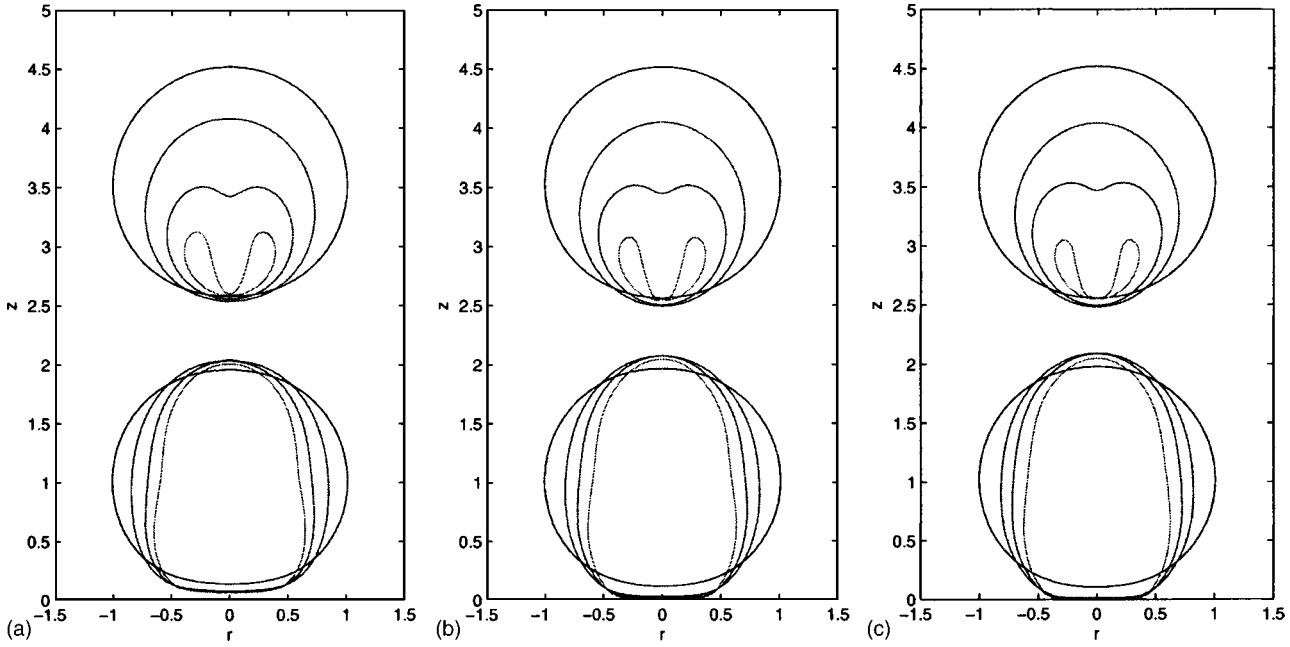

FIG. 16. (Color online) Bubble profiles for $R_{1m}=R_{2m}=1$, $\gamma_1=3.5$, $\gamma_2=1$, and $R_{01}=R_{02}=0.2$ during the collapse phase. From outermost to innermost: (a) $\beta=0$, $t=1.088, 1.896, 2.101, 2.209$; (b) $\beta=0.05$, $t=1.037, 1.826, 1.993, 2.111$; (c) $\beta=0.1$, $t=0.986, 1.752, 1.898, 2.021$.

make the two cavities approach to each other more), make the downward liquid jet of the upper cavity wider, and make the upward liquid jet of the lower cavity develop more before the jet impact of the upper cavity happens.

It can be seen from Figs. 16 and 17 that in case 6, during the collapse phase surface tension effects make the centroid of the upper cavity move downwards more and make its downward liquid jet wider. In this case surface tension has no significant effect on the behavior of the lower cavity.

It can be seen from Figs. 18–21 that in case 7 and case 8, surface tension effects make the centroid of the upper cavity move downwards more and its downward liquid jet smaller.

IV. CONCLUSIONS AND DISCUSSIONS

By including surface tension effects and neglecting buoyancy force effects the behavior of two cavities growing and collapsing axisymmetrically near a rigid wall have been simulated numerically by boundary integral method. From the numerical results we can draw the following conclusions.

Surface tension will resist the deformation of a cavity and make it closer to spherical during its growth phase, and make it collapse faster.

For the case where the two cavities are nearly equal, during the collapse phase, surface tension effects will make the centroid of the upper cavity move downwards more and its downward liquid jet wider; will make the centroid of the lower cavity move upwards more and its upward liquid jet develop more if the two cavities are close to each other and far away from wall; and will make the centroid of the lower cavity elongated more in vertical direction if it is near the wall and far away from the upper cavity.

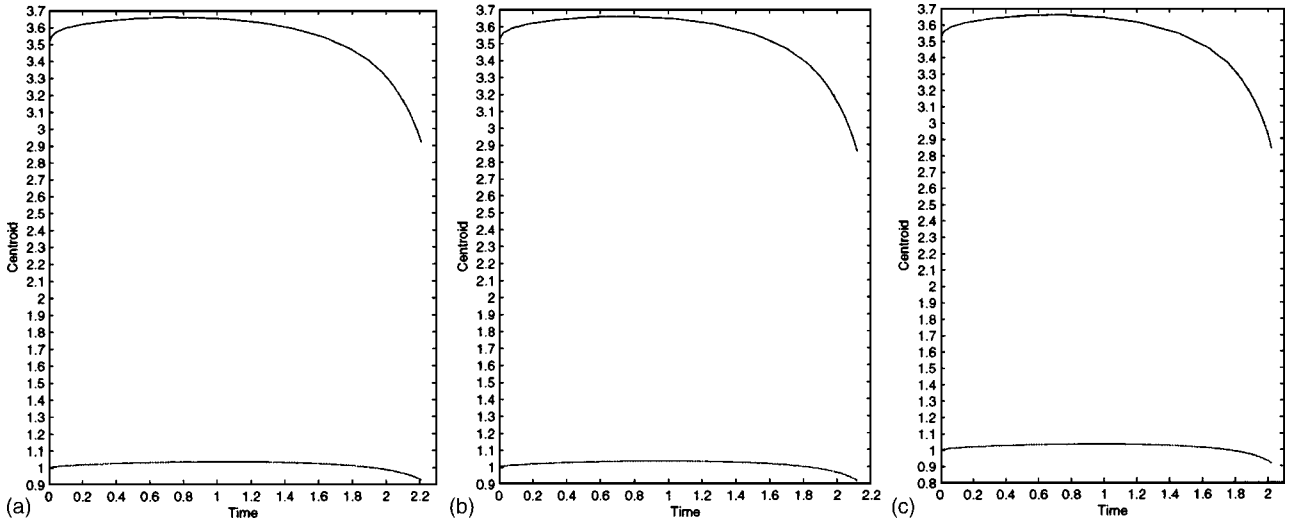

FIG. 17. (Color online) Centroid positions of the bubbles corresponding to the case of Fig. 16. (a) $\beta=0$, (b) $\beta=0.05$, and (c) $\beta=0.1$.

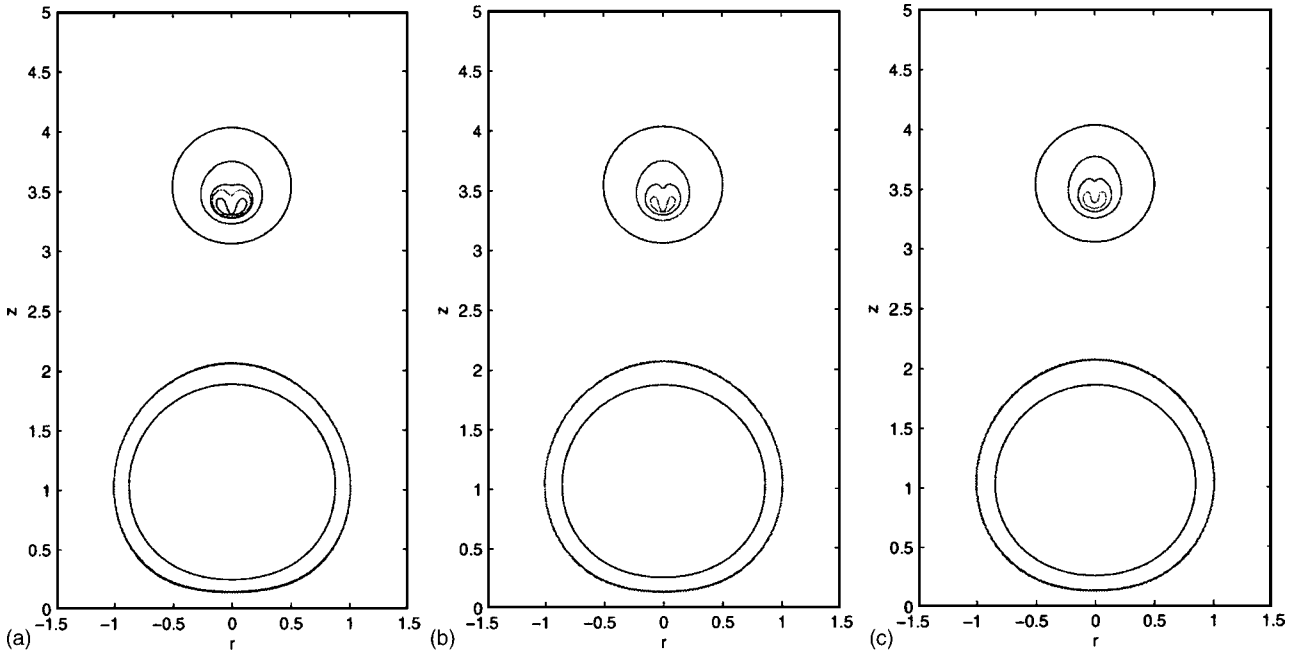

FIG. 18. (Color online) Bubble profiles for $R_{1m}=1$, $R_{2m}=0.5$, $\gamma_1=1$, $\gamma_2=3.5$, $R_{01}=0.2$, and $R_{02}=0.1$ during the collapse phase. From outermost to innermost: (a) $\beta=0$, $t=0.507, 1.007, 1.050, 1.057, 1.068$; (b) $\beta=0.05$, $t=0.445, 0.904, 0.933, 0.943$; (c) $\beta=0.1$, $t=0.401, 0.817, 0.843, 0.853$.

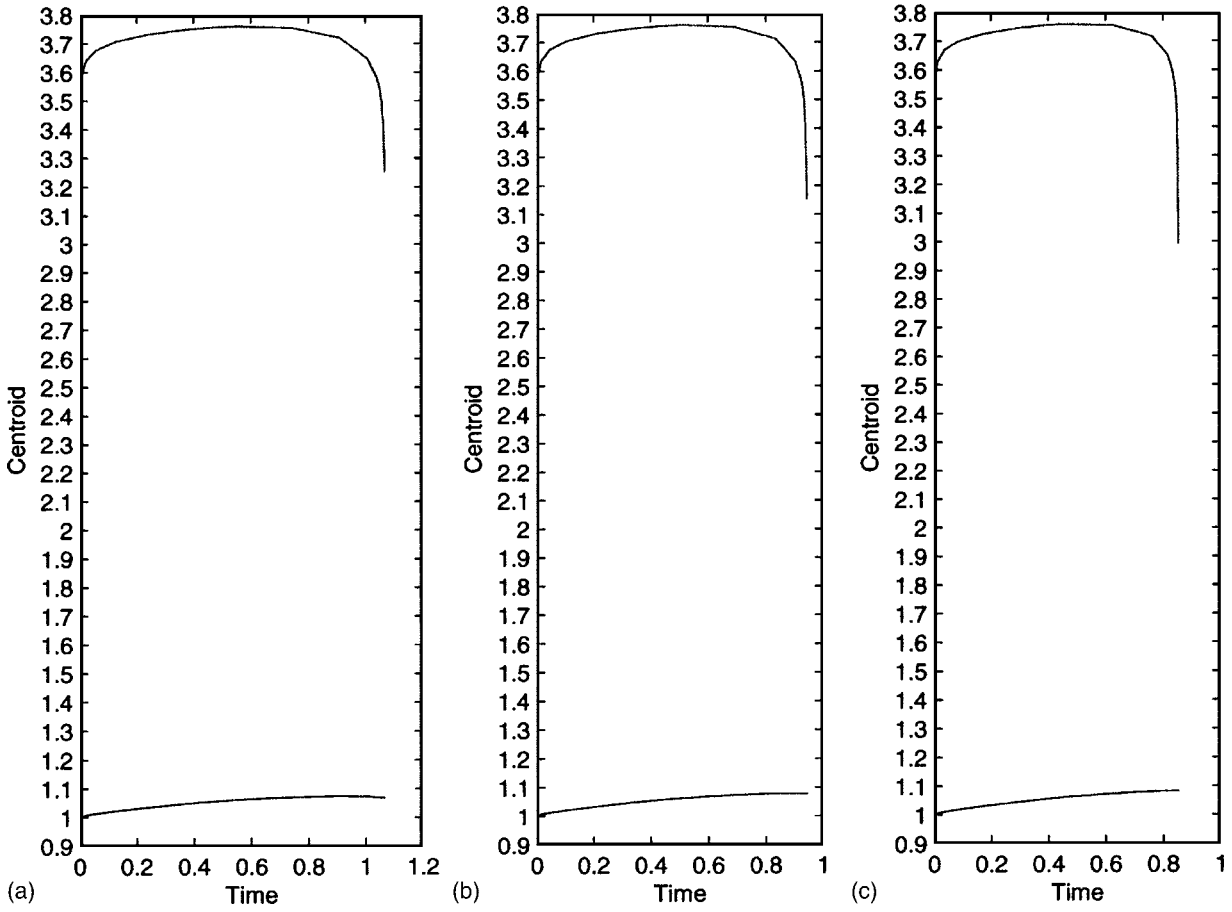

FIG. 19. (Color online) Centroid positions of the bubbles corresponding to the case of Fig. 18. (a) $\beta=0$, (b) $\beta=0.05$, and (c) $\beta=0.1$.

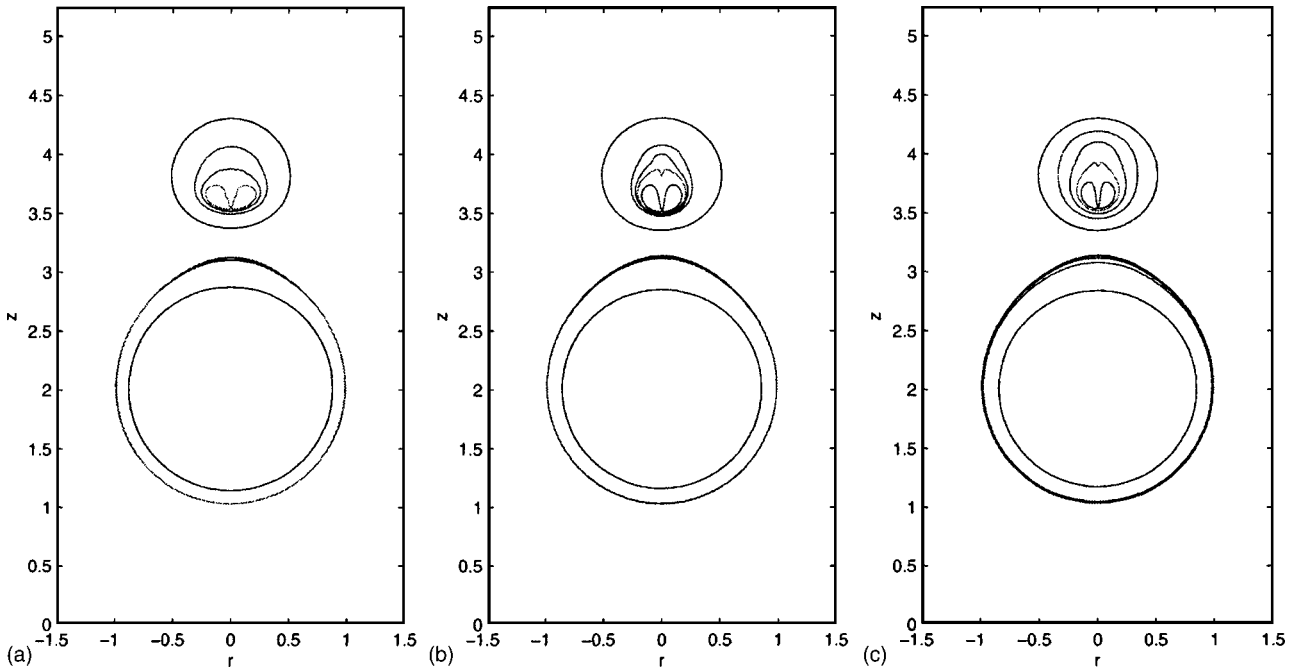

FIG. 20. (Color online) Bubble profiles for $R_{1m}=1$, $R_{2m}=0.5$, $\gamma_1=2$, $\gamma_2=3.75$, $R_{01}=0.2$, and $R_{02}=0.1$ during the collapse phase. From outermost to innermost: (a) $\beta=0$, $t=0.519,1.018,1.075,1.105$; (b) $\beta=0.05$, $t=0.448,0.923,0.950,0.961,0.979$; (c) $\beta=0.1$, $t=0.405,0.763,0.830,0.859,0.873$.

If one cavity is much smaller than the other, surface tension will not have significant effect on the behavior of the larger cavity.

When the upper cavity is much smaller than the lower one, during the collapse phase, surface tension effects will make the centroid of the upper cavity move downwards more and its downward liquid jet smaller.

For the case where the lower cavity is much smaller than the upper one, during the collapse phase, surface tension effects will strengthen the Bjerknes force to the lower cavity

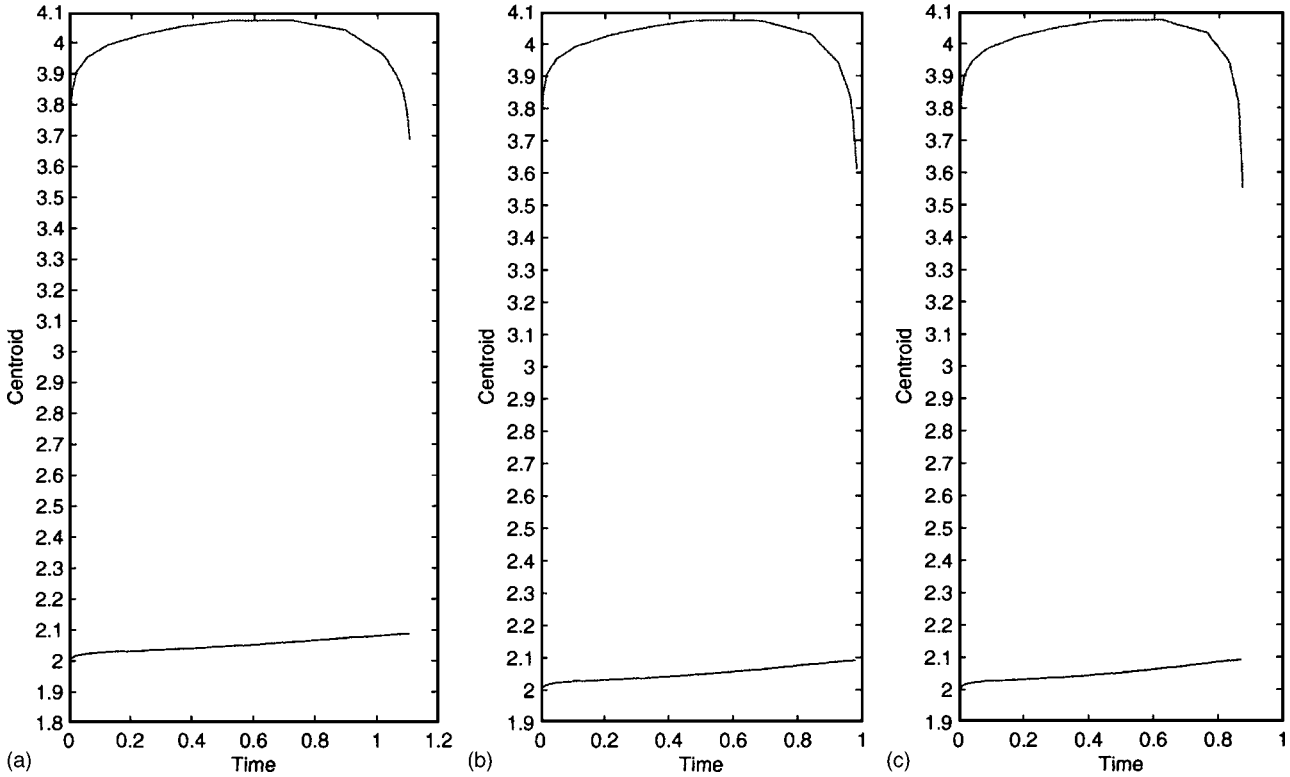

FIG. 21. (Color online) Centroid positions of the bubbles corresponding to the case of Fig. 20. (a) $\beta=0$, (b) $\beta=0.05$, and (c) $\beta=0.1$.

induced by the wall and weaken that induced by the upper cavity. Therefore surface tension effects will make the centroid of the lower cavity move downwards more and its downward liquid jet wider if the lower cavity is near the wall and far away from the upper one; will make the centroid of the lower cavity move upwards less and its upward liquid jet thinner if the lower cavity is near the upper one and far away from the wall; and will play a dominant role in the behavior of the lower cavity such as change the direction of its liquid jet from annular to downward or from upward to annular and then to downward.

For a convex cavity, surface tension has the action of resisting the cavity deformation during its growth phase and the action of accelerating the cavity deformation during its collapse phase. This is similar to those induced by Δp. The phenomena induced by surface tension effects can be explained by this mechanism.

ACKNOWLEDGMENT

This work was supported by NSFC Project No. 10272032.

[1] J. R. Blake, B. B. Taib, and G. Doherty, J. Fluid Mech. **170**, 479 (1986).
[2] J. P. Best and A. Kucera, J. Fluid Mech. **245**, 137 (1992).
[3] J. P. Best, J. Fluid Mech. **251**, 79 (1993).
[4] S. Zhang, J. H. Duncan, and G. L. Chahine, J. Fluid Mech. **257**, 147 (1993).
[5] J. R. Blake, P. B. Robinson, A. Shina, and Y. Tomita, J. Fluid Mech. **255**, 707 (1993).
[6] K. Sato and Y. Tomita, in *Third International Symposium on Cavitation*, Grenoble, France, edited by J. M. Michel and H. Kato (Universite Joseph Fourier, Grenoble, 1998), Vol. 1, pp. 63–68.
[7] S. Rungsiyaphornrat, E. Klaseboer, B. C. Khoo, and K. S. Yeo, Comput. Fluids **32**, 1049 (2003).
[8] Z. Zhang and H. Zhang, Phys. Rev. E **70**, 056310 (2004).
[9] A. H. Stroud and D. Secrest, *Gaussian Quadrature Formulas* (Prentice Hall, Englewood Cliffs, NJ, 1966).
[10] A. Harten, S. Osher, B. Engquist, and S. Chakravathy, J. Comput. Phys. **71**, 231 (1987).